Journal of Structural Geology, Vol. 11, No. 5, pp. 523 to 538, 1989
Printed in Great Britain

0191-8141/89 $03.00 + 0.00

Structural development during flysch basin collapse: the Fencemaker allochthon, East Range, Nevada

MARK W. ELISON and ROBERT C. SPEED

Department of Geological Sciences, Northwestern University, Evanston, IL 60208, U.S.A.

(*Received* 28 *September* 1988; *accepted in revised form* 21 *February* 1989)

Abstract—During Mesozoic deformation in north-central Nevada, a thick succession of Triassic siliciclastic and hemipelagic carbonate strata that were deposited in a deep-water basin shortened against and overrode penecontemporaneous shallow-water carbonates and interbedded siliciclastics at the eastern margin of the basin. Initial rheologic contrasts developed between lithologic units during shallow pretectonic burial localized displacements within fine-grained, poorly-cemented units and along lithologic boundaries. Changes in rheology during low-pressure and low-temperature deformation led to more brittle conditions, possibly due to fluid expulsion, and subsequent displacements truncated bedding. Structures in Triassic strata suggest that the W-facing slope of the shelf-to-basin transition localized thrusting. Collapse of the basinal strata against strata of the basin margin and formation of a thrust at the shelf-to-basin transition demonstrate the ability of stratigraphic declivities and associated rheologic contrasts to buttress deformation and localize thrusting.

INTRODUCTION

THEORETICAL analysis has emphasized the importance of material parameters in all aspects of thrust fault development (Mitra & Boyer 1986). Rheologic control of thrust fault geometry is evident from the observations that prominent basal décollements often develop at the contact between stratigraphic cover and crystalline basement rocks (Price 1981, Dixon 1982, Woodward 1982) and that thrust faults often parallel bedding in incompetent units and ramp across competent units leading to classic staircase geometry (Dahlstrom 1970, Royse *et al.* 1975). In continuous parallel-layered stratigraphic sequences, rheology is a primary constraint on the localization and geometry of thrust faults, but variations in stratigraphic layering that occur at facies boundaries, basin margins or pre-existing structures also influence thrust fault development (Beutner 1977, Knipe 1985, Kopania 1985). In cases where both rheologic and geometric perturbations occur, for example at steps in basement topography, the potential for thrust fault localization has been theoretically demonstrated (Wiltschko & Eastman 1983, Schedl & Wiltschko 1987).

Shelf-to-basin transitions, particularly at continental margins, provide a setting for dramatic rheologic variation and associated irregularities in stratigraphic layering due to discontinuities of units at the slope, facies changes and non-horizontal depositional surfaces. The common observation within many orogenic belts that oceanic basement and affiliated sediments are thrust above or structurally imbricated with continental margin strata (Kligfield *et al.* 1981, Speed & Sleep 1982, Monger *et al.* 1985, Brown *et al.* 1986, Price 1986, Dietrich 1988) demonstrates the potential of the continental margin-oceanic basin transition to localize displacement.

During Mesozoic deformation in north-central Nevada, the Jurassic Fencemaker thrust (Fig. 1) emplaced a thick allochthon of Triassic basinal flysch above penecontemporaneous carbonate and siliciclastic strata at a late Triassic shelf-to-basin slope. We present an analysis of the structures in Triassic strata juxtaposed across the Fencemaker thrust. Structures in the Triassic strata provide insight into the kinematics of collapse of basinal strata against the slope, the mechanisms of shortening in the basinal strata, the influence of initial rheology on deformation mechanisms and of deformation mechanisms on rheology, and the response of basin margin strata to contraction.

Important results are that the Triassic shelf-to-basin slope provided stratigraphic slip surfaces that localized displacement zones in both allochthon and autochthon to the Fencemaker thrust. The geometry of the slope allowed younger strata to be thrust above older strata, and controlled the fault–fold relationships in the allochthon. Changes in the rheology of strata, primarily due to fluid expulsion, eliminated preferred lithologic displacement zones and subsequent faults propagated across lithologic contacts.

REGIONAL STRUCTURAL SETTING

The Fencemaker thrust, located in the western Great Basin, is an extensive feature within the Mesozoic Winnemucca deformation belt. The Winnemucca deformation belt is the westernmost of three belts of Mesozoic imbrication: the Winnemucca belt, the Eureka belt and the Sevier belt (Speed *et al.* 1988) (Fig. 1). At its eastern boundary, the region of Mesozoic contraction overlaps the craton-shelf hinge that developed during late Precambrian rifting and formation of a passive margin to western North America (Stewart 1972, 1976). The region of Mesozoic deformation is bounded to the west by a continental magmatic arc that began in late Triassic

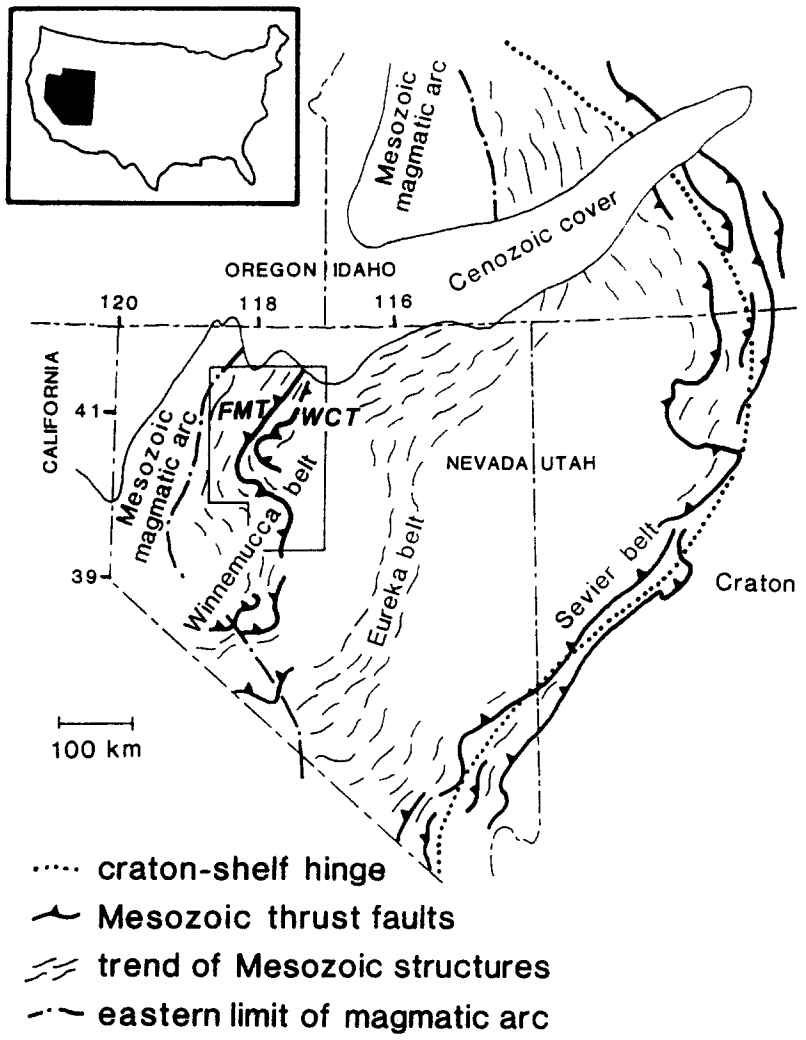

Fig. 1. Map of the Great Basin showing the distribution of Mesozoic tectonic elements and the location of the Winnemucca deformation belt. FMT is the Fencemaker thrust, WCT is the Willow Creek thrust. Box shows the area of Fig. 2. Inset shows the position of Fig. 1 within the western United States.

time and continued to form through the Cretaceous (Evernden & Kistler 1970, Chen & Moore 1982). At the latitude of northern Nevada, the arc developed outboard of the isotopically defined western edge of sialic North America (Kistler & Peterman 1973, 1978) upon a fragment of non-continental crust that became attached to North America in early Triassic time (Speed 1979).

The Winnemucca belt (Fig. 2) is composed of three contiguous N–S-trending fault-bounded packages: the Fencemaker allochthon, the Willow Creek allochthon and the Winnemucca belt autochthon. The Fencemaker allochthon is bounded to the W by W-verging folds and thrusts that juxtapose strata of the allochthon with rocks of the Mesozoic continental arc (Russell 1984, Maher & Saleeby 1988). The Fencemaker thrust forms the eastern margin of the Fencemaker allochthon. The Willow Creek thrust occurred after the Fencemaker thrust (Elison 1987) and emplaced the Willow Creek allochthon westward above Triassic strata that also compose the autochthon to the Fencemaker thrust. The geographic focus of this study is the northern East Range (Fig. 2) where one of few exposures of the Fencemaker thrust allows detailed kinematic analysis.

THE TRIASSIC STRATAL SEQUENCES

Over wide areas of the western Great Basin, Triassic strata are the youngest preserved Mesozoic deposits and provide the best record of subsequent deformation. Triassic strata within the Winnemucca deformation belt unconformably overlie a complex assemblage of Paleozoic North American shelf strata and allochthonous terranes that became attached to and overran the western margin of North America during the Mississippian Antler and earliest Triassic Sonoma orogenies (Silberling & Roberts 1962, Speed 1979, 1982). Two different but partially contemporaneous Triassic stratigraphic sequences occur within the Winnemucca deformation belt where they lie on either side of the Fencemaker thrust. Shallow-water Triassic strata accumulated at and east of the western edge of continental crust, and deep-water Triassic strata accumulated between the Mesozoic magmatic arc and the western edge of continental crust (Speed 1978a,b). The stratigraphy and interpretation of the depositional environments of these two sequences are summarized in Fig. 3(a) and discussed briefly below.

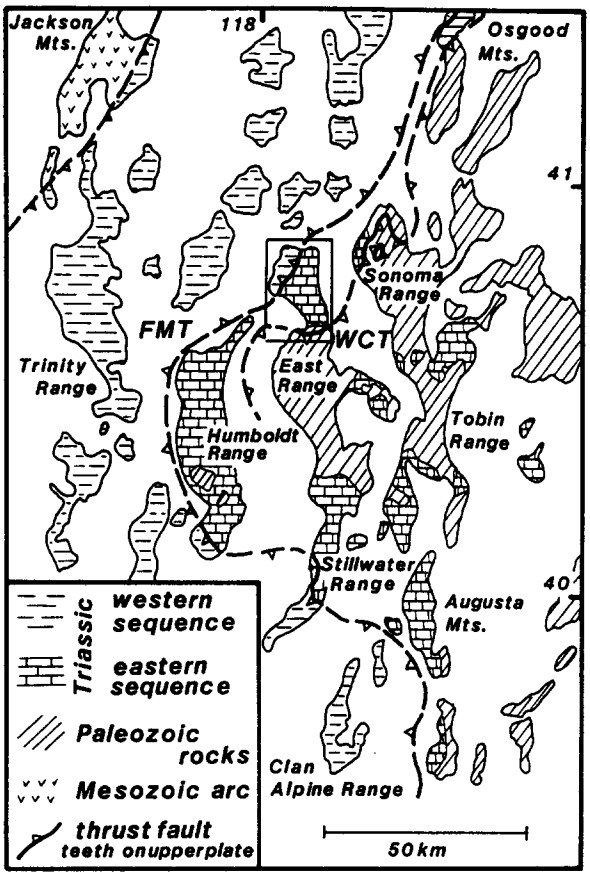

Fig. 2. Pre-Tertiary outcrop map of the Winnemucca thrust belt of north-central Nevada showing the position of the East Range and adjacent ranges with respect to the Fencemaker (FMT) and Willow Creek (WCT) thrusts. Box shows the area of Fig. 4.

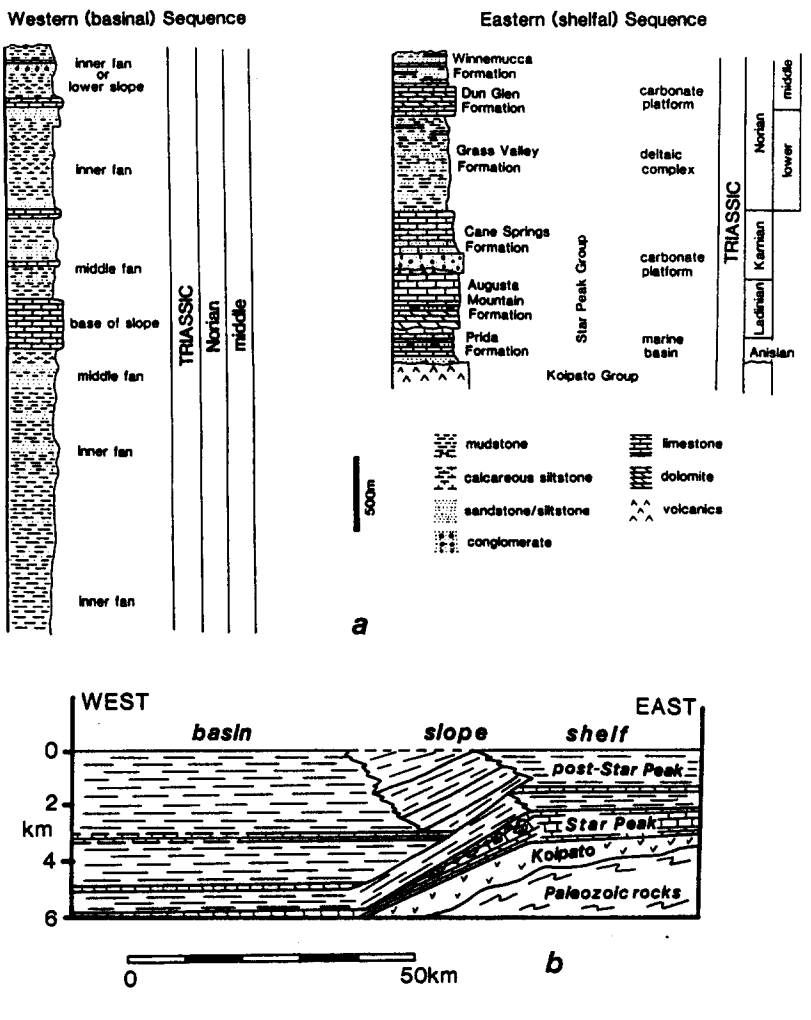

Fig. 3. (a) Stratigraphic columns, ages and interpreted depositional environments of the western Triassic sequence (Elison & Speed 1988) and the eastern Triassic sequence (Silberling & Wallace 1969, Nichols 1972, Nichols & Silberling 1977, Elison & Speed 1988) in the East Range. (b) Inferred configuration of Triassic strata in north-central Nevada at the end of the Triassic. Note that scales are approximate and that vertical exaggeration is large.

The eastern (shelfal) sequence

Siliceous volcanogenic rocks of the Koipato Group are the oldest rocks of the eastern sequence. The Koipato Group is unconformably overlain by the Triassic Star Peak Group, composed of shallow-water limestone and dolomite, interbedded siliciclastic sandstone, siltstone, and mudstone and local chert pebble conglomerate. The depositional environment of the Star Peak Group has been interpreted as a progradational carbonate platform punctuated by regressive and emergent periods (Silberling & Wallace 1969, Nichols & Silberling 1977). In Norian time, the Grass Valley, Dun Glen and Winnemucca Formations were deposited conformably atop the Star Peak Group. The Grass Valley Formation consists of interbedded siliciclastic sandstone, siltstone and mudstone interpreted to have been deposited as a deltaic complex (Silberling & Wallace 1969, Elison & Speed 1988). The Dun Glen Formation is shallow-water limestone and dolomite, similar to carbonate platform strata of the Star Peak Group. The Winnemucca Formation contains carbonate and siliciclastic strata that probably accumulated on a narrow shelf influenced by migration of siliciclastic and carbonate bars (Elison & Speed 1988). In the East Range, the eastern stratigraphic sequence is approximately 2 km thick, representing Anisian through middle Norian deposition (Fig. 3a). The platformal carbonates and deltaic strata record a long-lived, shallow-marine, shelf environment.

The western (basinal) sequence

Strata of the western Triassic sequence have been studied in a few areas (Speed 1978a, Heck & Speed 1987, Elison & Speed 1988) and have proven unamenable to stratigraphic correlation. At different locations, the sequence includes Triassic hemipelagic and pelagic strata, Norian terrigenous and calcareous flysch, local Lower Jurassic strata and the Jurassic Humboldt lopolith. Siliciclastic and calcareous flysch, transported by varied subaqueous processes (turbidity currents, debris flows and hemipelagic settling) to a deep marine environment, are the only strata of the western sequence in the East Range (Fig. 3a), where vertical layer sequences are indicative of migrating fan facies near a base of slope. The oldest exposed strata of the western sequence in the East Range are siliciclastic mudstones and channelized sandstones that record retrogradation of a submarine fan. These strata are overlain by hemipelagic carbonates that accumulated following abandonment of the fan. Younger parts of the sequence contain mixed component (carbonate + siliciclastic) strata deposited in a second submarine fan that prograded across the hemipelagic carbonates. Near the top of the exposed sequence, interbedded carbonate, conglomerate, and siliciclastic siltstone, mudstone and sandstone were deposited in lower slope or inner fan environments (Elison & Speed 1988).

Triassic paleogeography

Similar composition, partially contemporaneous deposition, and the preservation of an east to west, shallow- to deep-water facies transition, although tectonically foreshortened, suggest that the shelf and basinal sequences were initially continuous. Slope deposits representing depositional environments intermediate between the two sequences have been described locally (Silberling & Wallace 1969, Heck & Speed 1987). Paleogeographic reconstructions of north-central Nevada for late Triassic time (Heck & Speed 1987, Elison & Speed 1988) indicate that a west- and south-facing shelf-to-basin slope existed from early Ladinian through at least middle Norian time.

Onlap and offlap relationships of strata deposited at a slope can be predicted from retrogradational and progradational submarine fan facies (Brown & Fisher 1977, Schlager & Camber 1986). On the basis of exposed fan facies in the East Range, strata in the basin probably onlapped the slope during retrogradation of the early submarine fan and deposition of hemipelagic carbonate strata. Prograding deposits of the second submarine fan probably offlapped the hemipelagic carbonate strata. Figure 3(b) shows a model of the shelf-to-basin transition based on strata of the East Range. The eastern Triassic shelf sequence lies below the Fencemaker thrust whereas the western Triassic basinal sequence is everywhere above the Fencemaker thrust.

STRUCTURES IN TRIASSIC ROCKS OF THE EAST RANGE

In the East Range, the Fencemaker allochthon, the Fencemaker thrust, and the underlying autochthonous section are exposed (Fig. 4). Structures in Triassic strata record Mesozoic and younger deformation that includes emplacement of the Fencemaker allochthon. Paleozoic rocks of the region are highly deformed, but they contain no structures clearly related to the emplacement of the Fencemaker allochthon and apparently acted rigidly during that time. High-angle normal faults related to Basin and Range extension that occur throughout the East Range record relatively minor extension (Speed *et al.* 1988) and do not cause significant rotation of strata or earlier structures.

The Fencemaker allochthon

The Fencemaker allochthon exposed at the northwest corner of the East Range (Fig. 5) consists of five major fault-bounded packets and several smaller blocks. The allochthon has structural thickness of at least 3 km; the top is not exposed. Within the larger packets of the allochthon, four distinct groups of structures older than Basin and Range faulting are recognized (Elison 1987). The earliest deformation (D_1) consists of major and minor folds (F_1), that affect all strata of the allochthon, and fanned axial planar foliation (S_1). The second phase

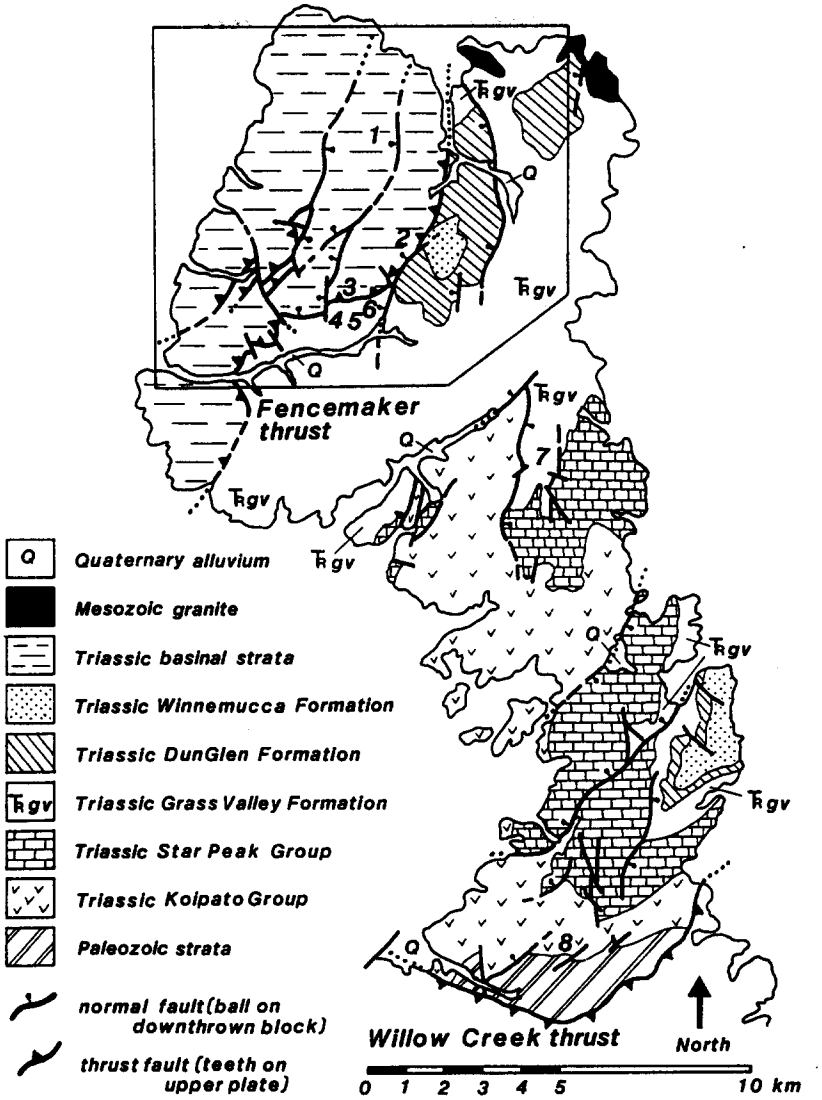

Fig. 4. Geologic map of the East Range showing the outcrop pattern of the eastern and western Triassic sequences and the positions of the Willow Creek and Fencemaker thrusts. Numbers give the positions of sample localities for strain measurements.

(D_2) includes reverse faults that truncate minor F_1 folds, F_2 folds that deform S_1, and local axial planar S_2 foliation. Shortening directions for D_1 and D_2, inferred from the orientation of folds, foliation and faults after removal of the effects of later deformation, trend ESE–WNW. A third phase of deformation (D_3), defined by folds (F_3) and associated foliation (S_3), deformed D_1 and D_2 fabrics. The orientation of D_3 fabrics suggests a shortening direction that trends nearly orthogonal to earlier shortening trends. Younger deformation in the allochthon includes low-angle normal faults, related folds (F_4), and high-angle Basin and Range normal faults.

The Triassic autochthon

The Triassic strata in the autochthon to the Fencemaker and Willow Creek thrusts (Fig. 4) are mainly upright and contain no major pre-Cenozoic faults. Syndepostional deformation (D_{0a}) occurs in the Grass Valley Formation and four subsequent phases of deformation are recognized (Elison 1987). The earliest tectonic deformation (D_{1a}) produced a foliation (S_{1a}) that is axial planar to rare, E-verging, tight to isoclinal F_{1a} folds. S_{1a} is folded by major and minor N–S-trending folds (F_{2a}), with axial planar S_{2a} foliation, that were reoriented and locally truncated during emplacement of the Willow Creek allochthon. Younger deformation post-dated emplacement of the Willow Creek allochthon and included scattered conjugate folds (F_{3a}) and normal faults that truncate earlier fabrics. Structures related to the Willow Creek thrust developed without reactivation or destruction of structures related to the Fencemaker thrust, and differentiation of Willow Creek and Fencemaker structures is not complicated.

FENCEMAKER ALLOCHTHON EMPLACEMENT STRUCTURES

Early deformation within the Winnemucca deformation belt resulted in an estimated 50–70% ESE–WNW

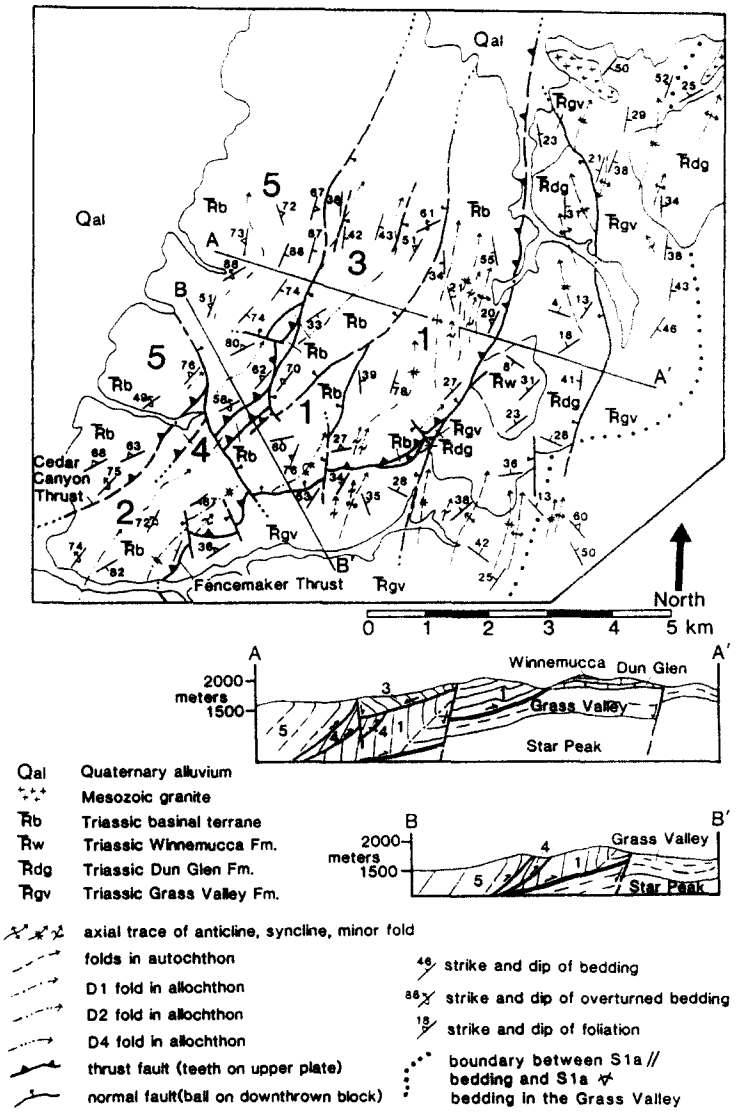

Fig. 5. Geologic map and cross-sections of the northernmost East Range showing the Fencemaker allochthon, Fencemaker thrust and a portion of the subjacent eastern Triassic sequence. Within the Fencemaker allochthon folds of different sets are distinguished by the number of dots in the dot–dash pattern of axial traces. D_{2a} fold axes are shown in the autochthon. Heavy dotted line delimits the boundary of the shear zone in the Grass Valley Formation. The other shear-zone boundary is the Fencemaker thrust. Numbers refer to the five major fault-bounded packages of the allochthon.

shortening of strata now in the Fencemaker allochthon on the basis of bed-length measurements in well exposed folds within the western sequence. This estimate does not take into account possible layer-parallel shortening, shortening due to foliation formation, or thrust displacement, and is thus probably a minimum. In the East Range, early ESE shortening trends within the allochthon are approximately normal to the Triassic shelf-to-basin transition, as determined by paleocurrent directions and the distribution of facies patterns in both shelf and basinal sequences (Silberling & Wallace 1969, Elison & Speed 1988). NNE displacement of the allochthon with respect to the autochthon (D_3) occurred after ESE displacement, indicated by superposed fabrics. D_3 folds deform E-verging reverse faults (D_2) in the allochthon of the East Range (Elison 1987) and E-verging shear zones (D_{1a}) in the autochthon of the Humboldt Range (Heck 1987). Collapse of basinal strata against the eastern basin margin and displacement of the western sequence to the ESE above the eastern sequence are, thus, represented by D_1 and D_2 structures within the allochthon.

S_{1a} is the earliest tectonic fabric in the autochthonous Triassic shelf sequence. N–S-trending folds (D_{2a}) that fold strata and early foliation (S_{1a}) in the autochthon also deform the Fencemaker thrust and both ESE- and NNE-verging structures in the Humboldt Range (Heck 1987) and the Stillwater Range. All later phases of deformation are synchronous with or post-date displacement on the Willow Creek thrust (Elison 1987). Only D_{1a} structures in the autochthon can be related to emplacement of the Fencemaker allochthon.

Early deformation (D_1) *in the allochthon*

The first fold phase of the Fencemaker allochthon (F_1) consists of a single close, ESE-overturned syncline that is only partially preserved, but greater than 3 km wide.

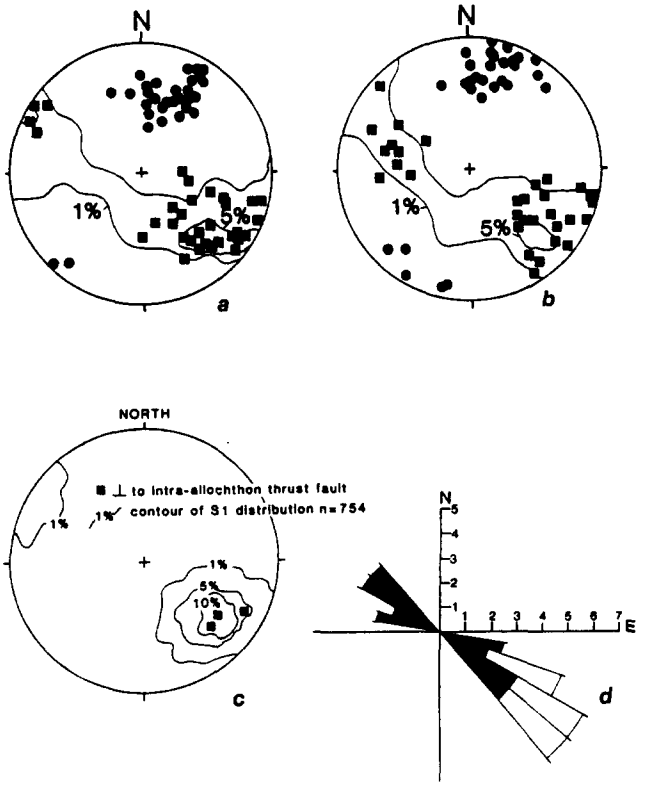

Fig. 6. Orientation data for D_1 and D_2 structures in the Fencemaker allochthon. (a) Fold axes (circles) and poles to axial planes (squares) of F_1 folds and contours of the distribution of poles to bedding in F_1 folds. (b) Fold axes (circles) and poles to axial planes (squares) of F_2 folds and contours of the distribution of poles to bedding and S_1 foliation in F_2 folds. (c) Contoured distribution of poles to S_1 foliation in the Fencemaker allochthon with, superimposed, poles to intra-allochthon thrust faults demonstrating their subparallel orientation. (d) Rose diagram of Fencemaker thrust displacement direction indicators. Filled area represents horizontal trend of X from finite-strain measurements and clast orientations, open area represents slip directions from foliation–fault intersections.

and involves all strata of the allochthon in the East Range. The axial plane of the major syncline strikes NNE and dips moderately WNW. Strata of the eastern, shallowly WNW-dipping, upright limb of the major syncline are subparallel to and above the Fencemaker thrust. Strata on the western, steep to overturned limb are truncated by the thrust (Elison & Speed 1988) forming a hangingwall truncation in excess of 2 km normal to the strike of hangingwall bedding (Fig. 5). Parasitic, tight, minor folds, 5–40 cm wide and 10–100 cm in amplitude, occur in mud-rich layers on both limbs of the major syncline. Where they are not refolded, minor folds have steeply to moderately WNW-dipping axial planes and fold axes that form a partial girdle in the axial plane with predominant shallow NNE and SSW plunge (Fig. 6). Minor F_1 folds show layer thickening in hinge regions with hinge thickness 150–400% of limb thickness. Commonly F_1 minor folds approximate class 2 folds (Ramsay 1967, p. 367). Single surface shapes of minor folds have high limb-to-hinge ratios and narrow rounded hinges. The major syncline also has a narrow hinge region, but extensive faulting and lack of exposure prohibit analysis of single surface shape or layer thickness variation.

Axial planar foliation (S_1) in fine-grained siliciclastic units defines a divergent fan. On major fold limbs the foliation is subparallel to bedding and up to 20° oblique to the major fold axial plane. S_1 intensity varies as a function of lithology and distance from the Fencemaker thrust trace. Within 1500 m of the thrust trace, the foliation is penetrative in muddy rocks and fine-grained carbonates and spaced in medium- to coarse-grained carbonates, siltstones and sandstones. Farther away, S_1 remains penetrative in muddy rocks, but is spaced and anastomosing in carbonates, and absent in sandstones. Clasts in conglomerate, near the thrust trace, are flattened in the plane of the S_1 foliation and have elliptical shapes on the foliation surface. S_1 is defined by preferred orientation of detrital and authigenic phyllosilicates, preferred shape and orientation of quartz and carbonate grains, and spaced selvages composed of phyllosilicates and opaque material. Foliae are 0.3–1 mm thick zones of 0.01–0.001 mm thick discontinuous anastomosing selvages that truncate quartz and carbonate grains with straight contacts; grain size is generally reduced in selvage zones. Areas between selvage zones vary from 0.1 to 4 mm wide. Where penetrative, the foliation is defined by the shape and orientation of clastic grains and growth of phyllosilicates between selvages. Asymmetric beards of crystalline calcite on detrital grains, and rare calcite and quartz filled veins perpendicular to the foliation indicate local reprecipitation of some material removed from selvage zones. Selvages, from which quartz, rock fragments and feldspar were entirely removed, are pervasive whereas veins of quartz are rare, thin and discontinuous suggesting that the amount of quartz precipitated locally was less than that removed from selvage zones and implying volume loss from the local rock system. Discordances of S_1 at contacts between carbonate layers and fine-grained siliciclastic or mixed carbonate–siliciclastic layers suggest that layer-parallel displacements of probably small magnitude occurred throughout the allochthon.

The fabric associated with D_1 deformation is well developed throughout the allochthon. S_1 and F_1 are pervasive and appear to represent the dominant episode of strain experienced by the basinal strata. All fabrics related to later deformation episodes, including D_2, are sporadically developed and locally absent.

Progressive deformation (D_2) *in the allochthon*

Two major reverse faults occur within the allochthon: the Cedar Canyon thrust and a reverse fault approximately 500 m east (Fig. 5). Both strike NNE and dip 65–75° WNW. The faults are subparallel to the S_1 foliation (Fig. 6) and truncate bedding on the steep to overturned limb of the major F_1 syncline. Gentle to close F_2 folds are upright to ESE-overturned with shallowly NNE-plunging axes and partial girdle axial plane distribution about the fold axis (Fig. 6). F_2 folds are E-verging on both limbs of the major F_1 fold.

F_2 folds occur in two spatially restricted domains; they are of different size and geometry in each. Above the

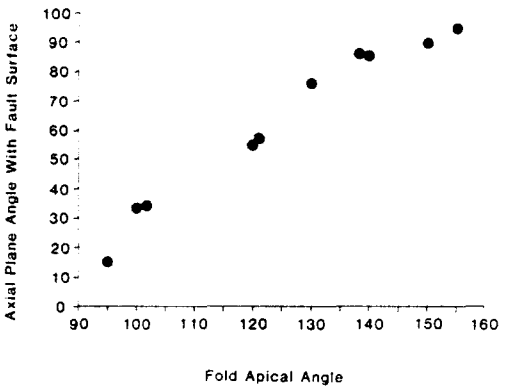

Fig. 7. Graph of the relationship between apical angle and axial plane orientation of D_2 folds that occur in the walls of D_2 intra-allochthon reverse faults. Rotation of intermediate fold limbs results in tighter folds and migration of the axial plane toward the fault surface.

Fencemaker thrust near its trace, F_2 folds occur in a wavetrain on the upright F_1 fold limb (Fig. 5) and are from 25 to 100 m in amplitude and width. They are asymmetric, rounded hinged, class 1B folds. F_1 minor folds are inverted on the southeast limbs of F_2 folds, indicating SE vergence of F_2. A spaced planar foliation (S_2), axial planar to F_2 folds, is defined by sharp hinged crenulations of S_1 spaced 1–20 mm apart (average 7 mm). No selvages or indications of fluid mobility or volume loss are associated with S_2. F_2 folds are also developed in the walls of reverse faults within the allochthon, on the steep F_1 fold limb, where they are 10–200 cm in amplitude, 50–400 cm in width and occur as isolated fold pairs. These are asymmetric narrow-hinged folds that have thickened short limbs relative to long limbs and no axial planar foliation. Axial planes to F_2 folds that are spatially associated with intra-allochthon reverse faults dip steeply to moderately WNW or ESE, and a relationship exists between the tightness and orientation of the folds; the angle between the axial plane and the proximal fault surface and the apical angle of the fold are proportional (Fig. 7). D_2 structures, in contrast to D_1, are spatially restricted and appear to be dominated by localized failure and associated high shear strain concentrated at fault surfaces.

Interpretation of allochthon structures

The basinal strata of the Fencemaker allochthon in the East Range locally had a burial depth >2 km, indicated by the thickness of hangingwall strata truncated by the thrust. At depths of >1.5 km, normally compacted fine-grained siliciclastic rocks have a porosity of <0.2, and at depths of 3 km porosity is reduced to <0.1 (Baldwin & Butler 1985). No disrupted strata, sandstone dikes or diapirs, or other evidence of overpressuring are observed in the allochthon in the East Range and normal compaction curves are probably applicable. Siliciclastic siltstones and sandstones have sutured grain contacts and rare quartz overgrowths, both truncated by S_1 selvage zones, indicating that these strata underwent compaction and cementation prior to tectonism. Medium-grained carbonates and fine-grained, clean (>95% $CaCO_3$) carbonates developed neomorphic blocky spar or equigranular microspar during diagenesis. In medium–coarse-grained siliciclastic units and carbonates, both cementation and neomorphic crystal formation are known to occur at shallow burial depths (Mazzullo 1981, Wescott 1983, Machemer & Hutcheon 1988, Malenaar *et al.* 1988, Smosna 1988), consistent with reconstructions of allochthonous strata.

The observed dependence of S_1 intensity on lithology is inferred to be a function of the initial sedimentologic and diagenetic history of basinal strata. Development of S_1 in most lithologies was by pressure solution. In siliciclastic mudstone pervasive growth of phyllosilicates may have post-dated pressure solution, indicated by concentrations of authigenic phyllosilicates in selvage zones. Pressure solution is favored by fine grain size and presence of clay particles or insoluble residue and is inhibited by cementation (Westcott 1983, Marshak & Engelder 1985, Houseknecht 1988, Mitra 1988). Correlation of remnant diagenetic fabrics and S_1 intensity suggests that siliciclastic sandstones and clean carbonates were more competent than finer grained, mixed component strata and siliciclastic mudstone during D_1. The competency contrast is indicated by the observation that mixed component siltstones have closely spaced to penetrative pressure-solution foliation, whereas coarse carbonate fragments replaced by neomorphic blocky spar display little or no pressure solution and have deformed by calcite twinning.

Interbeds of competent and incompetent units will deform harmonically if competent units are sufficiently closely spaced (Ramsay 1967, p. 417). The harmonic development of the F_1 major fold in all strata of the allochthon indicates that some basinal strata were strong enough to deform coherently. Although the western sequence is well stratified on a scale of 10–100 cm, the only thick, continuous, competent unit is the 300 m thick carbonate section (Fig. 3). Because the clean carbonate of this unit was more competent than surrounding fine-grained siliciclastic and mixed component rocks during D_1, it may have approximated a single viscous layer in a less viscous medium. For such single layer folds, initial wavelength to thickness ratios depend on the viscosity contrast between the layer and its matrix and decrease during layer-parallel shortening at limb dips <10–20° (Hudleston 1973b). If the F_1 syncline initiated as a plane strain sinusoidal buckle due to layer-parallel compression, then, neglecting body forces and using the relationship of Hudleston (1973b), the 300 m thickness of the carbonate unit and >3 km wavelength of the F_1 syncline imply that the viscosity contrast between the carbonate section and enclosing mudstone was >50:1.

All the fault-bounded packets of the allochthon contain parasitic F_1 minor folds and S_1 foliation that is axial planar to F_1 in the hinge regions of both major and minor folds, but defines a divergent fan in mudstones. The divergent cleavage fan indicates that folding included layer-parallel simple shear on fold limbs, a conclusion supported by S_1 refraction at layer contacts. Divergent

cleavage fans in incompetent units are typical of foliation resulting from combinations of tangential longitudinal strain and layer-parallel simple shear (Ramsay 1967, pp. 403–405) as in the case of flexural slip folds. The lack of evidence for slip parallel to axial planes in the allochthon implies that the approximate class 2 style of F_1 folds resulted from flattening. Superposed flattening with maximum shortening perpendicular to the axial plane of a fold modifies any initial geometry toward class 2, with changes in bed thickness that are dependent on the angle of dip of bedding and the superposed flattening strain (Ramsay 1967, p. 413). The divergent cleavage fan and layer thickness variations in folds suggest that F_1 folds developed by flexural slip and were modified by either contemporaneous or superposed flattening. The ubiquitous evidence for pressure solution during S_1 foliation development suggests that flattening was likely accommodated by volume loss normal to S_1.

In an attempt to quantify the strain associated with bedding-parallel simple shear and flattening, R_f and ϕ measurements were made of quartz grains in three samples of fine-grained mixed component clastic rocks from the Fencemaker allochthon. Three thin sections were cut from each sample and for each thin section the shape and orientation of at least 50 quartz grains were measured. None of the samples contained S_2 crenulations. Analytic methods of two-dimensional strain determination by Shimamoto & Ikeda (1976) and Robin (1977) were applied to the R_f and ϕ values for each section and gave consistent results. The three-dimensional finite strain was determined by the method of Gendzwill & Stauffer (1981). The locations of the samples for which finite-strain measurements were made are shown in Fig. 4 and the results are given in Table 1. For the samples from the allochthon, the calculated finite strains are in the oblate field (Fig. 8) and have k values less than 0.2.

The divergence of selvages around clastic quartz grains in these samples indicates that the quartz grains were less soluble than surrounding material. Therefore, the finite strain indicated by quartz grain shapes developed during pressure solution is likely less than finite strain in the matrix. Moreover, because quartz grains did not deform homogeneously with their matrix, rigid rotation of quartz grains relative to the matrix may have occurred. The measured finite strain is predominantly a flattening strain, but there is no evidence for elongation parallel to X (i.e. $X \simeq Y > Z$ and $k \simeq 0$). Fold morphology and foliation relations indicate that both layer-parallel simple shear and flattening occurred, possibly contemporaneously. We suggest that during bedding-parallel simple shear quartz grains rotated such that their long and intermediate axes migrated towards the shear plane. Concomitant with rotation, pressure solution removed material from surfaces oriented normal to Z. Quartz grain shapes are interpreted to record primarily flattening strain. This interpretation allows that flattening and simple shear may have occurred contemporaneously during S_1 development, similar to a conclusion arrived at by Mosher (1980), who demonstrated that simple shear in a section of quartzite cobble conglomerates caused contemporaneous rotation and volume loss and resulted in oblate strain.

Superposed flattening normal to the axial plane of class 1B folds with $(1 + e_2)/(1 + e_1) \simeq 0.5$, the measured strain in quartz grains, would produce observed values of layer thickening in hinges relative to limbs at bed dips >60° (Ramsay 1967, p. 413). Although the axial plane of the major F_1 syncline is inclined to the horizontal, bedding on both limbs lies at an angle of ≈30° from the axial plane (equivalent to 60° bed dip for an upright fold). The relationships among measured strain, layer thickness variation, and the angle between bedding and the F_1 axial plane, suggest that flattening was normal to

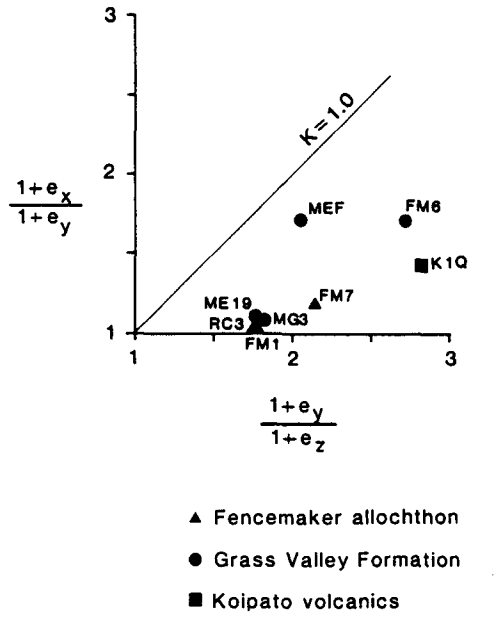

Fig. 8. Flinn plot of principal components of finite strain measured in clastic rocks of the Fencemaker allochthon, Grass Valley Formation and Koipato volcanics. Labels refer to sample designations given in Table 1.

Table 1. Finite strain in clastic rocks of the East Range. Principal components of finite strain, k values and grain size of samples from the Fencemaker allochthon, the Grass Valley Formation and the Koipato volcanics. The numbers of the samples refer to locations shown on Fig. 4. The sample designation refers to k values plotted in Fig. 8

Sample	$X:Y:Z$	k	Grain size
	Fencemaker allochthon		
(1) RC3	1.82:1.76:1.00	0.04	Silt
(2) FM1	1.85:1.79:1.00	0.05	Silt
(3) FM7	2.55:2.15:1.00	0.16	Silt
	Fencemaker autochthon		
Grass Valley Formation			
(4) FM6	4.66:2.71:1.00	0.42	Mud
(5) MEF	3.55:2.05:1.00	0.70	Mud
(6) MG3	1.98:1.83:1.00	0.10	Fine-grained sand
(7) ME19	1.98:1.76:1.00	0.16	Fine-grained sand
Koipato volcanics			
(8) K1Q	4.00:2.80:1.00	0.24	Conglomerate

the F_1 axial plane. Flattening normal to the axial plane is further suggested by the symmetry of layer thickness variation on opposing F_1 folds limbs. Similar results may occur for simultaneous buckling and flattening in the model of Hudleston (1973a), but finite-strain values are not uniquely defined by layer thickness variation as a function of bed dip, depending also on incremental rotations and flattening strains.

The current overturned attitude of the major F_1 syncline requires a component of rotation across the entire allochthon. The timing of rotation with respect to F_1 fold development and whether the rotation resulted from rotational strain (e.g. top-to-the-ESE simple shear) or rigid rotation are unclear. Possible causes for the overturned attitude of the F_1 syncline are discussed below in the interpretation of the Fencemaker thrust.

S_1 foliation is folded in F_2 folds spatially associated with intra-allochthon reverse faults and the reverse faults are not folded in F_1 folds, indicating that folding in the major F_1 syncline occurred prior to the formation of packet-bounding faults and prior to F_2 folds. The orientation and sense of short limb rotation of F_2 folds are compatible with displacement to the southeast between S40°E and S80°E, roughly equivalent to the Fencemaker slip direction (Fig. 6). F_2 fold axes are approximately colinear with local F_1 minor fold axes. Poles to refolded F_1 axial planes, bedding, and S_1 foliation that are folded in F_2 form partial girdles that are coplanar with bedding girdles due to F_1 (Fig. 6). These relationships suggest that F_1 and F_2 folds were generated in non-coaxial progressive deformation with clockwise rotation of the X and Z strain axes ($X > Y > Z$) about a N-plunging Y axis. Moreover, the relationship between tightness and orientation of F_2 folds spatially associated with intra-allochthon reverse faults (Fig. 7) suggests that the folds formed due to inhomogeneous simple shear adjacent to the faults (Sanderson 1979). This relationship, the compatibility of F_2 short limb rotation and fault vergence, and the spatial association of F_2 folds and faults indicate that the intra-allochthon faults and F_2 folds were cogenetic and that the folds are due to top-to-the-east simple shear parallel to the faults. ESE translation of strata occurred within the allochthon during D_2 by formation of reverse faults and F_2 folds and is compatible with continued displacement on the Fencemaker thrust.

We conclude that the Fencemaker thrust was active during D_1 and D_2 deformation and that F_2 folds and the intra-allochthon faults followed D_1 in a progressive non-coaxial deformation with ESE–WNW-trending X and a component of top-to-the-ESE simple shear. On the steep limb of the D_1 syncline, progressive strain was accommodated by reverse faulting in areas of thick carbonate layers. Near the Fencemaker thrust on the upright synclinal limb, progressive strain was accommodated by refolding of the early fabric in siliciclastic mudstone sections. It is probable that both orientation of layering on the limbs of the D_1 syncline and layer composition and thickness contributed to the contrast of deformation mechanisms. Loss of porosity and fluid pressure during D_1 may have precluded continued flattening by volume loss and may also have decreased the rheologic differences between layers, such that bedding no longer provided preferential slip surfaces, allowing D_2 faults to truncate bedding.

Early deformation (D_{1a}) *in the autochthon*

D_{1a} in the autochthon is defined by a foliation (S_{1a}) that is variably developed as a function of lithology and position. Tight to isoclinal, E-verging F_{1a} folds with axial planar S_{1a} foliation are restricted to small areas at the base of the Star Peak Group in southeastern exposures. S_{1a} is defined by phyllosilicate preferred orientation, selvages of clay and opaque material, and preferred shape and orientation of ellipsoidal clastic grains. S_{1a} is penetrative and planar in muddy and tuffaceous rocks, spaced and anastomosing or absent in carbonates, and spaced or absent in sandstones.

In the Grass Valley Formation S_{1a} is planar and penetrative to thinly spaced (1 mm) in mudstones and spaced (1 cm) in sandstones. Within approximately 1.7 km horizontal distance from the Fencemaker thrust trace (Fig. 5), the S_{1a} foliation in mudstones lies at an angle of up to 30° from bedding. The angle between S_{1a} and bedding in mudstones decreases with increasing distance from the Fencemaker thrust trace and farther than 1.7 km from the thrust trace S_{1a} is parallel to bedding. The sense of obliquity is everywhere the same; S_{1a} dips WNW with respect to horizontal bedding. Bedding-oblique and bedding-parallel foliation are never superposed and they occur in separate areas with a gradational boundary that parallels the trace of the Fencemaker thrust (Fig. 5). In sandstones S_{1a} is everywhere parallel or subparallel to bedding. The magnitude of strain associated with the S_1 foliation in the Grass Valley decreases with distance from the Fencemaker thrust trace. Near the trace, phyllosilicates in mudstones have near perfect preferred orientation. With distance from the thrust, the degree of preferred phyllosilicate orientation in mudstones decreases. Preferred optic orientation is less pronounced or absent in siltstones, fine-grained sandstones and mudstones distant from the Fencemaker thrust trace.

Throughout the Koipato Group, S_{1a} foliation is penetrative to thinly spaced and, where bedding can be determined, is parallel to bedding. A stretching lineation defined by grain elongation lies in the plane of the S_{1a} foliation. In conglomerates near the base of the Koipato, the foliation is defined by preferred clast shape and orientation and phyllosilicate growth in the matrix. In hand specimen, Koipato strata have only a single foliation, but microscopically two foliations occur at a low but variable angle to one another in a relationship that we interpret as an *S–C* fabric (Berthé *et al.* 1979, Lister & Snoke 1984). Dominant foliation surfaces, defined by 0.1 mm thick selvages of phyllosilicates and opaque material that have sharp contacts with quartz and feldspar grains, parallel bedding and define the mesoscopic foliation (S_{1a}). Grain size reduction is evident in

S_{1a} selvage zones. Stretching lineation and grain size reduction suggest that these are displacement (C) surfaces. S surfaces, defined by thin (0.01 mm) zones of phyllosilicate preferred orientation and 0.005 mm thick selvages of opaque material, are sigmoidal and oblique to C by 25–30° between C surfaces, but approach parallelism to C where the two surfaces merge. Asymmetric pressure shadows on quartz and feldspar grains and sigmoidal grain shapes suggest grain rotation occurred between C surfaces.

S_{1a} is commonly absent in other autochthonous Triassic strata, but locally developed in fine-grained siliciclastic strata of the Cane Springs and Winnemucca formations, in which case it is spaced and anastomosing, defined by preferred particle shape and orientation. The foliation is absent in conglomerates of the Cane Springs Formation and sandstones of the Winnemucca Formation. Although S_{1a} is locally penetrative in strata of the autochthon, it occurs with restricted distribution and much of the autochthon contains little or no fabric related to D_{1a} deformation.

Interpretation of autochthon structures

In the autochthon, initial stratigraphic burial depth prior to deformation is poorly constrained, but was likely greater than the 0–2 km thickness of preserved overlying shelf strata (Fig. 3a). The response of shelf strata to D_{1a} suggests a diagenetic history similar to that of strata in the allochthon. S_{1a} is absent in carbonate strata and spaced in siliciclastic sandstones, suggesting that carbonate layers and sandstone beds acted competently during deformation. Penetrative S_{1a} indicates that mudstones were incompetent during D_{1a} as were fine-grained strata of the allochthon.

In mudstones of the Grass Valley Formation, variation of S_{1a} attitude with respect to bedding as a function of distance normal to the Fencemaker thrust trace implies that foliation orientation was related to emplacement of the Fencemaker allochthon. In the Koipato Group, the stretching lineation, rare E-verging tight to isoclinal folds, and the S–C fabric suggest a component of E-verging simple shear during S_{1a} formation. The angular relationship between C and S surfaces is consistent with formation during top-to-the-east simple shear parallel to S_{1a} with maximum displacement gradient at the S_{1a} foliae. S_{1a} foliation in the Koipato and Grass Valley is inferred to be related to Fencemaker displacements.

Finite strain associated with S_{1a} in the Grass Valley and Koipato was measured to determine if the finite strain was compatible with simple shear. Strain measurements in the Grass Valley Formation, based on R_f,ϕ of quartz grains give X:Z ratios between 1.98 and 3.55 (Fig. 8, Table 1). Finite strain varies with lithology; sandstones have highly oblate strain with X:Z of approximately 2, whereas strain in mudstone is triaxial and has X:Z of 3.5. An estimate of finite strain in the Koipato (Table 1) was obtained from an outcrop of conglomerate that provided exposure surfaces orthogonal to the foliation and both parallel and orthogonal to the stretching lineation. The surfaces were taken to approximate the finite XZ and YZ planes, respectively. R_f for 25 clasts from each surface was measured. The harmonic mean (Babaie 1986) of the R_f values was calculated and the X:Y:Z ratio was determined as 4:2.8:1. The long axes of clasts (apparent finite X) trend NW–SE, as do local stretching lineations.

Simple shear cannot account for the orientation of S_{1a} foliation throughout the Grass Valley Formation. If S_{1a} was due entirely to bed-parallel simple shear, observed variations in S_{1a} orientation would suggest higher shear strain in sandstone than mudstone, and the angle between foliation and bedding would increase with increasing distance from the thrust due to diminished simple shear strain. The bedding-foliation angle, however, decreases with increasing distance from the thrust trace and measured strain is higher in mudstones than sandstones. The development of S_1 in siltstones and sandstones by pressure solution suggests that a combination of volume loss and simple shear may have produced S_{1a}. Bedding-parallel simple shear in mudstone bounded by sandstone layers in conjunction with vertical volume loss can explain the observed relationships. Where simple shear strain is zero, as in sandstones of the Grass Valley, volume loss produces a foliation parallel to horizontal bedding. Where simple shear occurred, as in mudstones, the foliation is inclined to horizontal bedding. Assuming two-dimensionsal strain and bedding-parallel simple shear followed by orthogonal volume loss, the variation in angle between horizontal bedding and foliation in mudstones as a function of both shear strain and volume loss can be calculated. Simple shear strain of 1.5 at the Fencemaker thrust, decreasing linearly to zero at 1.7–1.8 km east of the thrust trace and followed by vertical volume loss of 0.2–0.25, gives a good fit to the observed pattern (Fig. 9). This strain pattern accounts for the strain magnitude variation between mudstones and sandstones and highly oblate finite strain in sandstones as opposed to triaxial strain in mudstones. Patterns of variation in the angle between bedding and foliation produced by volume loss followed by or contemporaneous with simple shear are similar to patterns generated by simple shear followed by volume loss. If volume loss preceded or occurred synchronously with simple shear, however, higher shear strains than depicted in Fig. 9 would be required to produce the observed angles between bedding and foliation. Because a single fabric (S_{1a}) is present, rather than superposed fabrics generated by simple shear and volume loss, respectively, simple shear and volume loss may have occurred contemporaneously. S_1 foliation in the Grass Valley is interpreted to have resulted from top-to-the-east simple shear due to Fencemaker allochthon emplacement in conjunction with volume loss, possibly due to loading by the Fencemaker allochthon.

S_{1a} formation in the lower parts of the Star Peak Group and in the Koipato volcanics is also inferred to have resulted from simple shear, possibly with a component of volume loss. The S–C fabric in the Koipato is

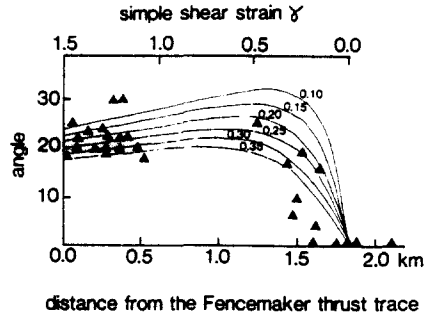

Fig. 9. Measured angles between bedding and S_1 foliation (triangles) in the Grass Valley Formation as a function of distance from the Fencemaker thrust trace, and predicted angles (solid lines) for model of bedding-parallel simple shear, with strain decreasing linearly with distance from the thrust trace, followed by vertical volume loss of 0.10–0.35 across the entire region. Volume loss preceding or synchronous with simple shear results in the same pattern but requires higher simple shear strains than depicted.

indicative of simple shear and the $k < 1$ triaxial strain (Fig. 8) suggests a component of pure shear or volume loss as well. Selvages partially define the S_{1a} foliation in the Koipato, and volume loss and simple shear may have occurred simultaneously. Pressure solution volume loss normal to C surfaces in S–C tectonites has been documented by Burg & Iglesias Ponce de Leon (1985).

S_{1a} records two discrete shear zones localized by lithology within the Grass Valley Formation and the Koipato volcanics. Carbonates and conglomerates of the Star Peak Group (Fig. 4) commonly lack early foliation and faults due to Fencemaker displacement are absent throughout the autochthon. Thus, no discontinuity developed and the thick-bedded and coarse-grained carbonates and conglomerates between the shear zones evidently underwent uniform eastward translation without thrusting. No method of determining the relative timing of S_{1a} development in the Grass Valley Formation and Koipato Group was discovered. It seems likely that the shear zone in the Koipato post-dated deformation of the Grass Valley Formation for reasons discussed below, but the two zones may have been contemporaneous.

The Fencemaker thrust

The trace of the Fencemaker thrust on topography in the northern East Range, although offset across several N–NW-trending normal faults, indicates that the thrust dips shallowly to the WNW over approximately 8 km (Fig. 5). The Fencemaker thrust is the easternmost thrust fault related to collapse of the flysch basin and emplaces a >3 km section of flysch above the autochthon. The total thickness of the allochthon is unknown and may have included the entire 6 km+ thickness (Speed 1978a) of the western Triassic sequence. Normals to the intersection of the thrust surface with fault related foliation near or at the thrust trace indicate slip between S49°E and S68°E (Fig. 6). The trend (horizontal component) of the long axis of conglomerate clasts is between S38°E and S53°E, subparallel to the Fencemaker thrust slip direction. The finite XZ ($X > Y > Z$) plane suggested by the axis and axial plane orientations of D_1 and D_2 fold strikes approximately S60°E. The parallelism of the trend of the thrust slip direction and finite X, and the orthogonal orientation of fold axes suggests that the allochthon traveled ESE up the dip of the Fencemaker thrust.

The Fencemaker thrust juxtaposed strata deposited near but on opposite sides of the late Triassic shelf-to-basin slope. The thrust has a slip direction roughly orthogonal to the slope and facies foreshortening suggests that displacement need not have been great. The thrust lies subparallel to bedding in the Grass Valley Formation but cuts the Dun Glen and Winnemucca(?) Formations at a low angle forming a footwall ramp approximately 300 m normal to stratigraphic layering (Fig. 5). The implication of the footwall ramp is that pieces of the Dun Glen and Winnemucca were incorporated into the allochthon at some point and have since been removed either tectonically or by erosion. This footwall ramp gives the Fencemaker thrust a ramp-flat geometry with respect to footwall bedding. Given the geometry of the slope depicted in Fig. 3(b), the hangingwall truncation (Fig. 5) may have resulted either from ramping of the thrust within basinal strata or from ramping of the thrust along an onlapped unconformity at the slope. In the latter case, the thrust may have everywhere paralleled footwall bedding, and a footwall truncation complementary to the hangingwall truncation need not exist.

Interpretation of the Fencemaker thrust

Early in the deformational history of the allochthon, zones and/or surfaces of displacement occurred within lithologic units and followed lithologic boundaries. During pressure solution and formation of S_1 in the allochthon, advective fluid flow is suggested by removal of material from the local rock system, following the arguments of Engelder & Marshak (1985). The presence of substantial amounts of fluid, largely confined to specific lithologic units, decreases friction and normal stress favoring displacement localization within those units. In contrast, D_2 reverse faults truncate carbonate units and are marked by zones of brecciation suggesting that these faults occurred under drier, more brittle, conditions.

S_{1a} in the Grass Valley Formation and S_1 in the allochthon formed under comparable conditions, indicated by similar morphology and the necessity for advective fluid flow. Pressure-solution foliation in the Grass Valley and the allochthon are interpreted to have formed contemporaneously. The shear zone recorded by S_{1a} in the Grass Valley extends beneath the Dun Glen Formation (Fig. 5) and the carbonates of the Dun Glen, undeformed during D_{1a}, must have been translated to the east above the shear zone. No thrust exists between the Dun Glen and Grass Valley and this shear zone may

have been a zone of ductile deformation propagating forward of the thrust. Where the Fencemaker thrust cuts the Dun Glen Formation, the Dun Glen is heavily fractured and carbonates in the adjacent allochthon are brecciated. This brittle deformation is similar to D_2 intra-allochthon reverse faults, and we propose that truncation of the Dun Glen by the Fencemaker thrust occurred synchronously with reverse faulting in the allochthon. These conclusions imply that the Fencemaker thrust had a two-stage history with early displacement under conditions of abundant fluid and later displacement under more brittle, drier conditions. The two stages may have been progressive with ductile deformation and dewatering propagating ahead of brittle failure.

The relationship between the initiation of F_1 folds and the Fencemaker thrust is poorly constrained because no change in orientation of the thrust is observed and because the anticlinal hinge of the F_1 fold is eroded. The elements that may allow differentiation of fault–fold relations (Jamison 1987) are, thus, limited. The existence of the hangingwall truncation (Fig. 5) and the lack of F_1 folding of the Fencemaker thrust indicate that the F_1 syncline formed prior to or synchronously with Fencemaker thrusting. If the thrust and fold developed contemporaneously, the fold may have been an accommodation to variation in the thrust geometry. Alternatively, it may have taken up displacement above a detachment and since been truncated. Both models provide for truncation of hangingwall strata but in the fault accommodation model ramping of the thrust and folding occur contemporaneously (Suppe 1983) whereas in the detachment fold model (Jamison 1987) initiation of the fold precedes thrust ramping. Both models also account for rotation of the F_1 fold to its current overturned orientation, either by fault-bend folding as the allochthon accommodated a change in thrust geometry or by simple shear produced by drag (Berger & Johnson 1980) or variations in slip and propagation rate (Williams & Chapman 1983) on a planar thrust.

S_1 is inferred to be contemporaneous with the early stage of Fencemaker thrust development and to have developed during flattening of F_1 folds. The implication is that S_1 formed after initiation of F_1. This interpretation is similar to one of Boulter (1979), who described a section of arenites, wackes and slates in which two foliations formed during folding. The second foliation that he described was defined by preferred dimensional orientation of detrital grains and mica flakes and was interpreted to have developed by pressure solution during flattening of folds after they attained interlimb angles of approximately 100°. The second foliation of Boulter (1979) is remarkably similar to S_{1a} in the Fencemaker allochthon and in both areas quartz grains have low axial ratios relative to qualitative strain and a divergent cleavage fan developed in slates. If S_1 developed synchronously with Fencemaker thrust formation and late in the development of F_1 folds, then F_1 folds probably initiated prior to early thrust displacement as in the case of detachment folding (Jamison 1987). Although both S_1 and early thrust development may have been prolonged and overlapped in time, we favor a model of F_1 development as a detachment fold.

MODEL OF BASIN COLLAPSE

A model of Fencemaker allochthon displacement is shown in Fig. 10. The model assumes that the Triassic stratigraphy of the region prior to deformation (Fig. 10a) was that shown in Fig. 3(b). During early subhorizontal contraction of the basinal strata, the Fencemaker thrust formed a basal detachment above which F_1 folds initiated (Fig. 10b). This detachment was probably a zone of concentrated simple shear, rather than a discontinuity, localized between lithological contacts by local fluid abundance. The geometry of the slope may have provided lithologic conduits for fluids as in the situation described by Elverhoi & Gronlie (1981). We submit that as simple shear in slope strata, equivalent in age to the Grass Valley Formation, propagated forward of the thrust as fluids followed stratigraphic boundaries at the slope and localized displacement (Fig. 10c). Development of F_1 folds restricted to the allochthon requires that displacements at the slope were less than displacements within the basin, suggesting that the slope buttressed early deformation and implying that the Fencemaker thrust propagated from within the basin toward the slope. During continued contraction, the Fencemaker thrust ramped with respect to the horizontal, parallel to footwall bedding, along an onlapped unconformity at the slope (Fig. 10c). F_1 folds were flattened and overturned by transpression at the thrust ramp and S_1 foliation formed. S_{1a} foliation formed synchronously in the Grass Valley Formation and continued to develop under conditions of bedding-parallel simple shear as the deformation zone propagated forward of the Fencemaker thrust tip (Fig. 10d). The boundary between allochthon and autochthon at this time was beneath the Dun Glen Formation and the Dun Glen migrated passively eastward above the Grass Valley shear zone and remained attached to the allochthon. Progressive deformation (D_2) occurred under increasingly brittle conditions as the allochthon was displaced up the slope along the Fencemaker thrust and fluids were expelled. At this stage, active displacement shifted from the Grass Valley shear zone to a ramp of the Fencemaker thrust across the Dun Glen Formation (Fig. 10e). The allochthon was displaced to the east with respect to currently exposed portions of the Grass Valley and Dun Glen Formations. Following or synchronous with final emplacement of the Fencemaker allochthon, footwall failure produced a second shear zone in the Koipato Group at the base of the Triassic stratal succession. Because the shear zone in the Koipato implies that displacement zones truncated stratigraphic units of the slope (Fig. 10e), we submit that the shear zone in the Koipato post-dated early stages of Fencemaker thrusting during which displacements were localized along rather than across stratigraphic horizons.

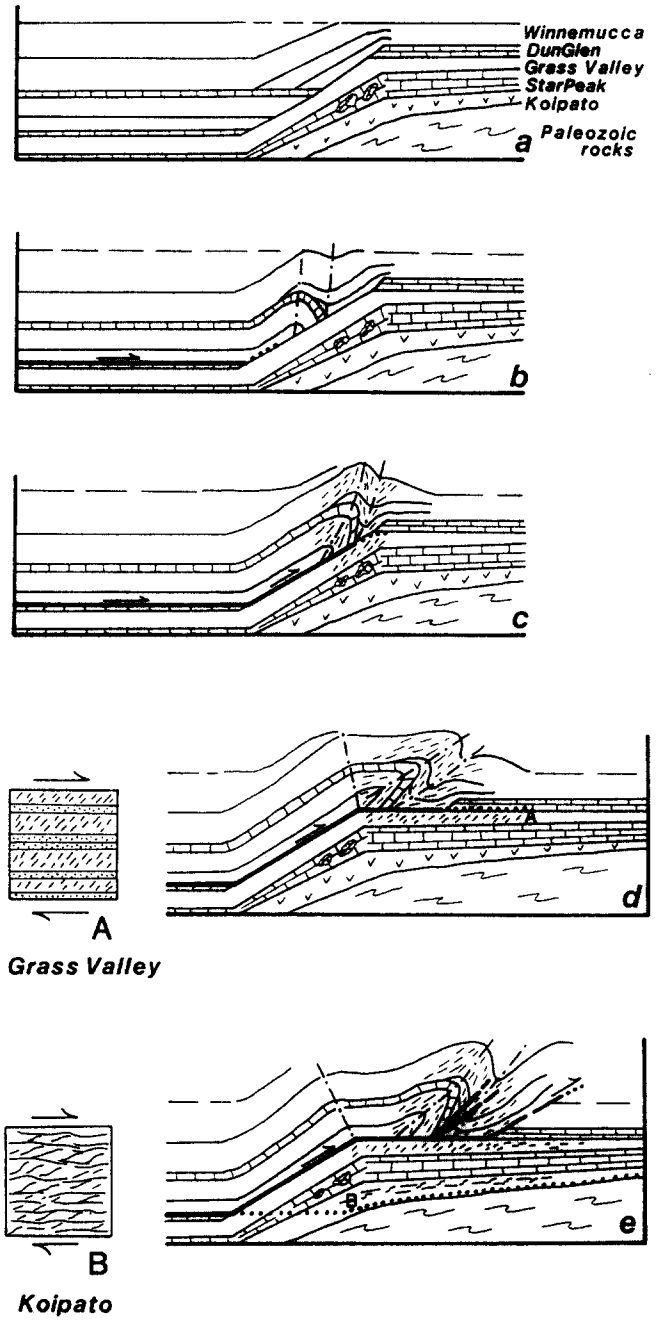

Fig. 10. Model of the development of Fencemaker structures in the East Range. Heavy lines are thrust faults, light lines are bedding, dashes are S_1 foliation in the allochthon and S_{1a} foliation in the autochthon, and dot–dash lines are axial traces to folds in the allochthon. (a) Pre-deformational configuration of Triassic strata and underlying late Paleozoic rocks. (b) Development of a detachment within the flysch basin and initial folding of the basin strata buttressed by the basin margin. Folds are only shown at the basin margin although they may have developed throughout the western sequence at this time. (c) Ramping of the Fencemaker thrust at the slope, formation of a hangingwall truncation without a correlative footwall truncation. S_1 and S_{1a} development occurs, as does flattening and contemporaneous overturning of allochthon folds by transpression at the ramp. (d) Translation of the hangingwall truncation forward of the ramp, development of a shear zone in the Grass Valley Formation and continued S_{1a} development and overturning of folds in the allochthon. (e) Development of D_2 thrusts during final emplacement of the Fencemaker allochthon, ramping of the Fencemaker thrust across the Dun Glen Formation, and development of the shear zone at the base of the eastern Triassic sequence. Boxes in lower left schematically show the development of simple shear zones for points A (Grass Valley shear zone) and B (Koipato shear zone) on model cross-sections (d) and (e), respectively.

CONCLUSIONS

(1) Early displacements within the Fencemaker allochthon were localized, by rheologic contrast, within fine-grained, poorly cemented stratigraphic units and at lithologic contacts.

(2) D_1 folds in the allochthon probably initiated to accommodate shortening above a shear zone or detachment parallel to lithologic contacts within or at the base of the flysch succession, and they were overturned and flattened during transpression at the basin margin when the thrust ramped with respect to the horizontal, parallel-to-footwall bedding, at the slope.

(3) Emplacement of the allochthon resulted in two zones of simple shear strain within the autochthon localized by rheology within stratigraphic units.

(4) Fluid loss during early deformation altered rheologic parameters and progressive deformation (D_2) during allochthon emplacement occurred under more brittle conditions allowing D_2 faults to truncate bedding.

(5) Diagenetic processes at shallow burial depth may produce rheologic contrasts between lithologic units and localize failure along rather than across bedding. Sloping lithologic contacts at basin margins may, consequently, localize ramping of detachments and produce out-of-the-basin displacements. Displacement parallel to bedding along an onlapped unconformity at the slope may result in hangingwall truncation in the absence of corollary footwall truncation.

Acknowledgements—This work was supported by National Science Foundation grant No. EAR-8519966 and by National Aeronautics and Space Administration grants Nos NAS5-27238A004 and NAG5-1008.

REFERENCES

Babaie, H. A. 1986. A comparison of two-dimensional strain analysis methods using elliptical grains. *J. Struct. Geol.* **8**, 585–587.

Baldwin, B. & Butler, C. O. 1985. Compaction curves. *Bull. Am. Ass. Petrol. Geol.* **69**, 622–626.

Berger, P. & Johnson, A. M. 1980. First-order analysis of deformation of a thrust sheet moving over a ramp. *Tectonophysics* **70**, T9–T24.

Berthé, D., Choukroune, P. & Jegouzo, P. 1979. Orthogneiss, mylonite and non-coaxial deformation of granites: the example of the South Armorican shear zone. *J. Struct. Geol.* **1**, 31–42.

Beutner, E. C. 1977. Causes and consequences of curvature in the Sevier orogenic belt, Utah to Montana. In: *Rocky Mountain Thrust Belt Geology and Resources* (edited by Heisey, E. L., Lawson, D. E., Norwood, E. R., Wach, P. H. & Hale, L. A.). *Wyoming Geol. Ass. Guidebook, 29th Ann. Field Conf.*, 353–365.

Boulter, C. A. 1979. On the production of two inclined cleavages during a single folding event; Stirling Range, S. W. Australia. *J. Struct. Geol.* **1**, 207–219.

Brown, L. F. & Fisher, W. L. 1977. Seismic-stratigraphic interpretation of depositional systems: examples from Brazilian rift and pull-apart basins. In: *Seismic Stratigraphy—Applications to Hydrocarbon Exploration* (edited by Payton, C. E.). *Mem. Am. Ass. Petrol. Geol.* **26**, 213–248.

Brown, R. L., Journeay, M., Lane, L. S., Murphy, D. C. & Rees, C. J. 1986. Obduction, backfolding and piggyback thrusting in the metamorphic hinterland of the southeastern Canadian Cordillera. *J. Struct. Geol.* **8**, 255–268.

Burg, J. P. & Iglesias Ponce De Leon, M. 1985. Pressure solution structures in a granite. *J. Struct. Geol.* **7**, 431–436.

Chen, J. H. & Moore, J. G. 1982. U–Pb isotopic ages from the Sierra Nevada batholith, California. *J. geophys. Res.* **87**, 4761–4785.

Dahlstrom, C. D. A. 1970. Structural geology in the eastern margin of the Canadian Rocky Mountains. *Bull. Can. Petrol. Geol.* **18**, 332–406.

Dietrich, D. 1988. Sense of overthrust shear in the Alpine nappes of Calabria (southern Italy). *J. Struct. Geol.* **10**, 373–381.

Dixon, J. S. 1982. Regional structural synthesis, Wyoming salient of western overthrust belt. *Bull. Am. Ass. Petrol. Geol.* **66**, 1560–1580.

Elison, M. W. 1987. Structural and tectonic history of the East Range, northcentral Nevada; implications for Mesozoic foreland tectonics. Unpublished Ph.D. Thesis, Northwestern University, Evanston, Illinois, U.S.A.

Elison, M. W. & Speed, R. C. 1988. Triassic flysch of the Fencemaker allochthon: fan facies and provenance. *Bull. geol. Soc. Am.* **100**, 185–199.

Elverhoi, A. & Gronlie, G. 1981. Diagenetic and sedimentological explanation for high seismic velocity and low porosity in Mesozoic–Tertiary sediments, Svalbard region. *Bull. Am. Ass. Petrol. Geol.* **65**, 145–153.

Engelder, T. & Marshak, S. 1985. Disjunctive cleavage formed at shallow depths in sedimentary rocks. *J. Struct. Geol.* **7**, 327–343.

Evernden, J. F. & Kistler, R. W. 1970. Chronology of emplacement of Mesozoic batholithic complexes in California and western Nevada. *Prof. Pap. U.S. geol. Surv.* **623**.

Gendzwill, D. J. & Stauffer, M. R. 1981. Analysis of triaxial ellipsoids: their shapes, plane sections and plane projections. *Mathematical Geol.* **13**, 135–152.

Heck, F. R. 1987. Mesozoic foreland deformation and paleogeography of the western Great Basin, Humboldt Range, Nevada. Unpublished Ph.D. Thesis, Northwestern University, Evanston, Illinois, U.S.A.

Heck, F. R. & Speed, R. C. 1987. Triassic olistostrome and shelf-basin transition in the western Great Basin: paleogeographic implications. *Bull. geol. Soc. Am.* **99**, 539–551.

Houseknecht, D. W. 1988. Intergranular pressure solution in four quartzose sandstones. *J. sedim. Petrol.* **58**, 228–246

Hudleston, P. J. 1973a. Fold morphology and some geometrical implications of theories of fold development. *Tectonophysics* **16**, 1–46.

Hudleston, P. J. 1973b. An analysis of "single layer" folds developed experimentally in viscous media. *Tectonophysics* **16**, 189–214.

Jamison, W. R. 1987. Geometric analysis of fold development in overthrust terranes. *J. Struct. Geol.* **9**, 207–219.

Kistler, R. W. & Peterman, Z. E. 1973. Variations in Sr, Rb, K, Na and initial Sr87/Sr86 in Mesozoic granitic rocks and intruded wall rocks in central California. *Bull. geol. Soc. Am.* **84**, 3489–3512.

Kistler, R. W. & Peterman, Z. E. 1978. Reconstruction of crustal blocks of California on the basis of initial strontium isotopic composition of Mesozoic granitic rocks. *Prof. Pap. U.S. geol. Surv.* **1071**.

Kligfield, R., Carmignani, L. & Owens, W. H. 1981. Strain analysis of a northern Apennine shear zone using deformed marble breccias. *J. Struct. Geol.* **3**, 421–436.

Knipe, R. J. 1985. Footwall geometry and the rheology of thrust sheets. *J. Struct. Geol.* **7**, 1–10.

Kopania, A. A. 1985. The effects of basement-cored buttresses and major stratigraphic changes on thrust sheets: an example from the Idaho–Wyoming–Utah thrust belt. *Geol. Soc. Am. Abs. w. Prog.* **17**, 249.

Lister, G. S. & Snoke, A. W. 1984. S–C mylonites. *J. Struct. Geol.* **6**, 617–638.

Machemer, S. D. & Hutcheon, I. 1988. Geochemistry of early carbonate cements in the Cardium Formation, central Alberta. *J. sedim. Petrol.* **58**, 136–147.

Maher, K. A. & Saleeby, J. 1988. Age constraints on the geologic evolution of the Jackson Mountains, NW Nevada. *Geol. Soc. Am. Abs. w Prog.* **20**, 177.

Malenaar, N., Van De Bilt, G. P., Van Den Hoek Ostende, E. R. & Nio, S. D. 1988. Early diagenetic alteration of shallow-marine mixed sandstones: an example from the lower Eocene Roda sandstone member, Tremp-Graus Basin, Spain. *Sediment. Geol.* **55**, 295–318.

Marshak, S. & Engelder, T. 1985. Development of cleavage in limestones of a fold-thrust belt in eastern New York. *J. Struct. Geol.* **7**, 345–359.

Mazzullo, S. J. 1981. Facies and burial diagenesis of a carbonate reservoir: Chapman Deep (Atoka) Field, Delaware Basin, Texas. *Bull. Am. Ass. Petrol. Geol.* **65**, 850–865.

Mitra, S. 1988. Effects of deformation mechanisms on reservoir potential in central Appalachian overthrust belt. *Bull. Am. Ass. Petrol. Geol.* **72**, 536–554.

Mitra, G. & Boyer, S. E. 1986. Energy balance and deformation mechanisms of duplexes. *J. Struct. Geol.* **8**, 291–304.

Monger, J. W. H., Clowes, R. M., Price, R. A., Simony, P. S., Riddihough, R. P. & Woodsworth, G. J. 1985. Continent–ocean transect B2; Juan de Fuca plate to Alberta plains. *Transects Program, Geol. Soc. Am.*

Mosher, S. 1980. Pressure solution deformation of conglomerates in shear zones, Narragansett Basin, Rhode Island. *J. Struct. Geol.* **2**, 219–225.

Nichols, K. M. & Silberling, N. J. 1977. Stratigraphy and depositional history of the Star Peak Group (Triassic), northwestern Nevada. *Spec. Pap. geol. Soc. Am.* **178**.

Price, R. A. 1981. The Canadian foreland thrust and fold belt in the southern Canadian Rocky Mountains. In: *Thrust and Nappe Tectonics* (edited by McClay, K. R. & Price, N. J.). *Spec. Publs geol. Soc. Lond.* **9**, 427–448.

Price, R. A. 1986. The southeastern Canadian Cordillera: thrust faulting, tectonic wedging, and delamination of the lithosphere. *J. Struct. Geol.* **8**, 239–254.

Ramsay, J. G. 1967. *Folding and Fracturing of Rocks*. McGraw-Hill, New York.

Robin, P. Y. F. 1977. Determination of geologic strain using randomly oriented strain markers of any shape. *Tectonophysics* **42**, T7–T16.

Royse, F., Jr., Warner, M. A. & Rees, D. L. 1975. Thrust belt structural geometry and related stratigraphic problems, Wyoming–Idaho–northern Utah. In: *Symposium on Deep Drilling Frontiers in the Central Rocky Mountains* (edited by Bolyard, D. W.). *Rocky Mountain Ass. of Geologists*, 41–55.

Russell, B. J. 1984. Mesozoic geology of the Jackson Mountains, northwest Nevada. *Bull. geol. Soc. Am.* **95**, 313–323.

Sanderson, D. 1979. The transition from upright to recumbent folding in the Variscan fold belt of southwest England: a model based on the kinematics of simple shear. *J. Struct. Geol.* **1**, 171–180.

Schedl, A. & Wiltschko, D. V. 1987. Possible effects of pre-existing basement topography on thrust fault ramping. *J. Struct. Geol.* **9**, 1029–1037.

Schlager, W. & Camber, O. 1986. Submarine slope angles, drowning unconformities, and self erosion of limestone escarpments. *Geology* **14**, 762–765.

Shimamoto, T. & Ikeda, Y. 1976. A simple algebraic method for strain estimation from deformed ellipsoidal objects. 1. Basic theory. *Tectonophysics* **36**, 315–337.

Silberling, N. J. & Roberts, R. J. 1962. Pre-Tertiary stratigraphy and structure of northwestern Nevada. *Spec. Pap. geol. Soc. Am.* **72**.

Silberling, N. J. & Wallace, R. E. 1969. Stratigraphy of the Star Peak Group (Triassic) and overlying lower Mesozoic rocks, Humboldt Range, Nevada. *Prof. Pap. U.S. geol. Surv.* **592**.

Smosna, R. 1988. Low-temperature, low-pressure diagenesis of Cretaceous sandstones, Alaskan North Slope. *J. sedim. Petrol.* **58**, 644–655.

Speed, R. C. 1978a. Basinal terrane of the early Mesozoic marine province of the western Great Basin. In: *Mesozoic Paleogeography of the Western United States* (edited by Howell, D. G. & McDougall, K. A.). *Soc. Econ. Paleont. Miner., Pacific Coast Paleogeography Symposium* **2**, 237–252.

Speed, R. C. 1978b. Paleogeography and plate tectonic evolution of the early Mesozoic marine province of the western Great Basin. In: *Mesozoic Paleogeography of the Western United States* (edited by Howell, D. G. & McDougall, K. A.). *Soc. Econ. Paleont. Miner., Pacific Coast Paleogeography Symp.* **2**, 253–270.

Speed, R. C. 1979. Collided Paleozoic microplate in the western United States. *J. Geol.* **87**, 279–292.

Speed, R. C. 1982. Evolution of the sialic continental margin in the central western United States. *Proc. Hedberg Conf. on Continental Margins. Mem. Am. Ass. Petrol. Geol.*, 457–468.

Speed, R. C., Elison, M. W. & Heck, F. R. 1988. Phanerozoic tectonic evolution of the Great Basin. In: *Rubey Volume 7, Metamorphism and Crustal Evolution of the Western United States* (edited by Ernst, G.). Prentice-Hall, New Jersey, 572–605.

Speed, R. C. & Sleep, N. H. 1982. Antler orogeny and foreland basin: a model. *Bull. geol. Soc. Am.* **93**, 815–828.

Stewart, J. H. 1972. Initial deposits of the Cordilleran geosyncline: evidence of a late Precambrian (850 my) continental separation. *Bull. geol. Soc. Am.* **83**, 1345–1360.

Stewart, J. H. 1976. Late Precambrian evolution of North America: plate tectonic implications. *Geology* **4**, 11–15.

Suppe, J. 1983. Geometry and kinematics of fault-bend folding. *Am. J. Sci.* **283**, 684–721.

Wescott, W. A. 1983. Diagenesis of Cotton Valley Sandstone (Upper

Jurassic), East Texas: implications for tight gas formation pay recognition. *Bull. Am. Ass. Petrol. Geol.* **67**, 1002–1013.
Williams, G. D. & Chapman, T. J. 1983. Strains developed in the hangingwall of thrusts due to their slip/propagation rate: a dislocation model. *J. Struct. Geol.* **5**, 563–571.
Wiltschko, D. & Eastman, D. 1983. Role of basement warps and faults in localizing thrust ramps. In: *Contributions to the Tectonics and Geophysics of Mountain Chains* (edited by Hatcher, R. D., Jr, Williams, H. & Zietz, I.). *Mem. geol. Soc. Am.* **158**, 177–190.
Woodward, L. E. 1982. Tectonic map of the fold and thrust belt and adjacent areas, west-central Montana. Montana Bureau of Mines and Geology Geologic Map 30.